Photoionization studies of GeH_n ($n=2$–4)

B. Ruscic, M. Schwarz, and J. Berkowitz
Chemistry Division, Argonne National Laboratory, Argonne, Illinois 60439

(Received 22 August 1989; accepted 9 October 1989)

The adiabatic ionization potential of GeH_4^+ (GeH_4) is measured by photoionization mass spectrometry to be $\leqslant 10.53$ eV and perhaps as low as 10.44 eV. This is about 0.8 eV (~ 9 vibrational quanta) lower than the value reported by photoelectron spectroscopy. This result, analogous to that found for SiH_4^+ (SiH_4), implies a marked Jahn–Teller distortion of GeH_4^+. The appearance potentials of GeH_2^+ and GeH_3^+ from GeH_4 are $\leqslant 10.77_2 \pm 0.009$ eV and $< 11.65_7 \pm 0.01$ eV, respectively. The reaction of F atoms with GeH_4 generates GeH_3, GeH_2 (weakly), and some atomic germanium. The adiabatic ionization potential of GeH_3 is $\leqslant 7.94_8 \pm 0.005$ eV; that of GeH_2 is $\leqslant 9.25$ eV. Together with auxiliary information, limits (more probable values) of the incremental bond energies, in kcal/mol, are found to be D_0 (H_3Ge–H) < 85.5 (82 ± 2); D_0 (H_2Ge–H) > 56.4 (59); D_0 (HGe–H) < 68.9 (66); and D_0 (Ge–H) > 53.7 (63). These specific bond energies, when appropriately normalized, display the same pattern as the SiH_n (but not the CH_n) bond energies and provide a basis for estimating the corresponding SnH_n bond energies.

I. INTRODUCTION

The paucity of experimental data on the bond strengths in the GeH_n system is astonishing, in view of the extensive use of GeH_4 in the semiconductor industry. Increased activity in recent years has clarified the thermochemistry of the corresponding SiH_n system[1] and the bond strengths in methane are rather well known.[2,3] However, in germane the available experimental data are limited to the GeH_3–H bond energy[4–7] and an upper limit to D_0 (GeH).[8] Even these values are not well established. The more recent results for the bond energy of GeH_3–H are 78.0 ± 1.0 kcal/mol[4] and 83 ± 2.4 kcal/mol.[5] Earlier values are $\leqslant 92.3 \pm 4.6$ kcal/mol[6] and 87.2 kcal/mol.[7] The upper limit for D_0 (GeH) ($\leqslant 3.3$ eV),[8] based on an observed predissociation[9] in the $A\,^2\Delta$ state is not a very useful upper limit, since D_0 (SiH) is 2.98 ± 0.03 eV[1] and one would expect D_0 (GeH) to be less than D_0 (SiH).

By contrast, accurate *ab initio* calculations, long limited to first and second row elements, have recently been applied to various aspects of the GeH_n problem. Balasubramanian and Li[10] have calculated the potential energy curves of several states of GeH, using multiconfiguration self-consistent field (MCSCF) with second-order configuration interaction (CI) and relativistic CI. They obtain D_e (GeH) = 2.81 eV and recommend $D_e = 2.85 \pm 0.05$ eV, based on comparison of their calculations with other experimentally established values. These numbers are equivalent to D_0 (GeH) = 2.70 or 2.74 ± 0.05 eV, well below the upper limit (3.3 eV) deduced spectroscopically.

Several papers[11–14] have focused their attention on the $X\,^1A_1$–$a\,^3B_1$ splitting in GeH_2, with calculated values ranging from 19.1 to ≈ 25 kcal/mol. The more recent separations obtained are 22.8[12] and 23.8[11] kcal/mol, slightly higher than in SiH_2.[1,15–17] However, no heats of formation or bond energies have been forthcoming from these calculations.

Within the past year, Kudo and Nagase[18] have calculated the most stable structure of GeH_4^+ and the minimum energy for decomposition of this parent ion into $GeH_2^+ + H_2$ and $GeH_3^+ + H$. Their calculations (MP4SDTQ/DZP + ZPC, fourth order Møller–Plesset perturbation theory including single, double, triple, and quadruple excitations, polarized double zeta basis set, with zero point energy corrections) lead to a highly Jahn–Teller distorted GeH_4^+ ground state, with C_s symmetry, approaching a $GeH_2^+ \cdot H_2$ complex. In fact, the dissociation energy to $GeH_2^+ + H_2$ is found to be only 4.9 kcal/mol, while the process forming $GeH_3^+ + H$ is computed to require 25.5 kcal/mol. These results are rather similar to the observations on SiH_4^+, both theoretical[19,20] and experimental.[1] Their calculated adiabatic ionization potential of GeH_4 (10.2 eV) is far below the value (11.3 eV) obtained from photoelectron spectroscopy.[21]

Our goal in the experimental work to be presented below was to determine the successive bond energies as hydrogen atoms are removed from GeH_4, by a combination of appearance potentials of fragment ions and adiabatic ionization potentials of the GeH_n ($n = 1$–3) free radicals. The method used to determine these quantities is photoionization mass spectrometry. Chemical reaction is used to generate the free radicals *in situ*. A further goal was to examine the onset energy of GeH_4^+ (GeH_4).

II. EXPERIMENTAL ARRANGEMENT

The basic photoionization mass spectrometric apparatus has been described previously.[22] A tight (more enclosed) ionization chamber was used for studies of stable GeH_4, while a more open chamber was employed for the free radical experiments. The chemical reaction used for generating the GeH_n radicals was hydrogen abstraction by fluorine atom interaction with GeH_4, analogous to an earlier study[1] of the products of the F + SiH_4 reaction. Additional experiments were performed using atomic hydrogen and atomic chlorine as reactants in an attempt to increase the yield of GeH_2, but these experiments were less successful.

III. EXPERIMENTAL RESULTS

Mass spectrometric studies with germanium compounds are more difficult than, e.g., silicon compounds, be-

 0021-9606/90/031865-11$03.00

cause of the wide distribution of isotopes. The isotopic abundances recommended by IUPAC (International Union of Pure and Applied Chemistry)[23] are M70 (20.5%), M72 (27.4%), M73 (7.8%), M74 (36.5%), and M76 (7.8%). This property causes overlap problems with different GeH_n^+ species and also reduces the effective abundance of any desired species. Hence, one must devise the most effective strategy for studying each particular species.

A. Photoionization of GeH_4

It is illustrative to compare the photoionization mass spectrum of GeH_4 with the He I photoelectron spectrum. In Fig. 1(a), the He I photoelectron spectrum of the first two (valence) bands[21] is reproduced. An overview of the photoionization mass spectrum (plotted on a photon energy scale, to conform to the photoelectron scale) is given in Fig. 1(b). In constructing this figure, GeH_4^+ was measured at the $m/e = 80$ position at shorter wavelengths, where contamination from other species was possible at other masses. To longer wavelengths, $m/e = 78$ and $m/e = 76$ were used. This strategy, while avoiding isotopic contamination, had the disadvantage that, when $m/e = 80$ was monitored, the inherently weak GeH_4^+ was reduced by more than an order of magnitude, since ^{76}Ge has a small isotopic abundance. The GeH_3^+ was monitored at $m/e = 77$, which is essentially isotopically pure and fairly abundant, until the threshold of GeH^+ (GeH_4). The GeH_2^+ species was measured at $m/e = 72$. The spectrum shown in Fig. 1(b) has been corrected for the various isotopic abundances and represents the fragmentation pattern of GeH_4. Comparison of Figs. 1(a) and 1(b) reveals that a weak but significant GeH_4^+ intensity in Fig. 1(b) extends well below ($\sim$0.8 eV below) the adiabatic threshold (11.3 eV) observed in the photoelectron spectrum (PES) [Fig. 1(a)]. Even the first fragment ion GeH_2^+ has its onset below 11.3 eV, but begins to increase significantly at approximately the adiabatic threshold observed in PES. The second fragment GeH_3^+ approaches the background level very gradually, even though its apparent onset occurs within the Franck–Condon region represented by Fig. 1(a).

1. GeH_n^+ (GeH_4)

The photoion yield curve of GeH_4^+ from GeH_4 is shown in greater detail in Fig. 2. Some rounded step structure is apparent as the curve approaches the threshold. There is some tailing very near to threshold, which may be due to a hot band, or to a very weak Franck–Condon factor. We choose the adiabatic threshold at 1178 Å $\equiv$ 10.53 eV, but it may be as low as 1188 Å $\equiv$ 10.44 eV. As mentioned earlier, this is $\gtrsim$0.8 eV below the adiabatic threshold observed in PES[21] (nine or ten vibrational quanta), but $\sim$0.3 eV higher than the value obtained by Kudo and Nagase.[18]

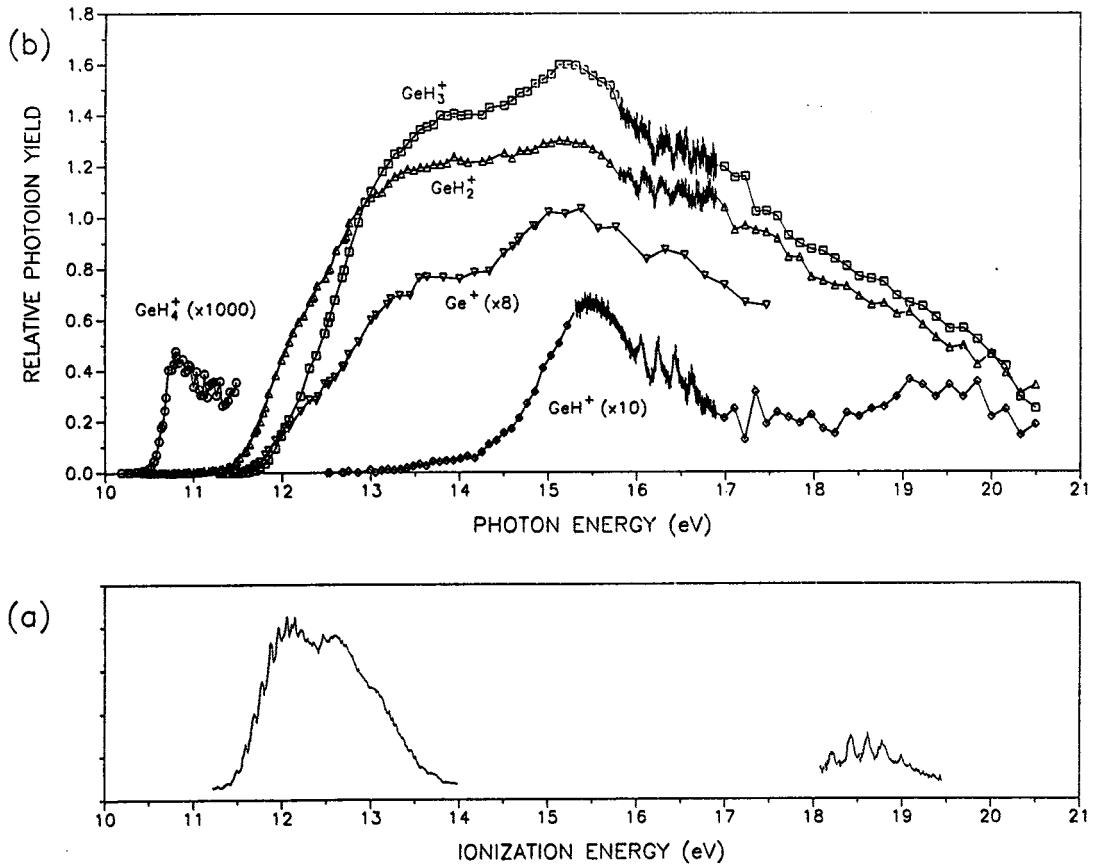

FIG. 1. (a) He I photoelectron spectrum of the first band of GeH_4 (from Ref. 21). (b) Photoion yield of the various GeH_n^+ species from GeH_4 as a function of photon energy. This spectrum has been corrected for isotopic abundance. O—GeH_4^+; □—GeH_3^+; Δ—GeH_2^+; ◇—GeH^+; ▽—Ge^+.

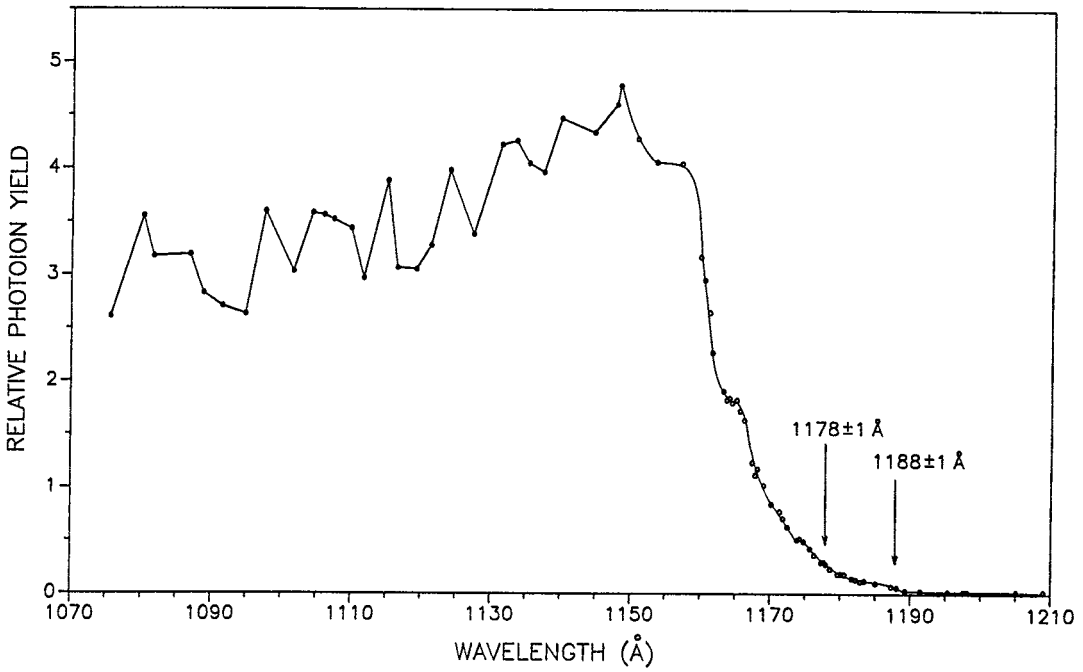

FIG. 2. The photoion yield curve of GeH_4^+ (GeH_4).

The steplike features in the GeH_4^+ have about the same spacing as the vibrational features in the photoelectron spectrum, which are observed at higher energy. The steplike features cease and the curve begins to decline below ~1160 Å, just where the first fragment (GeH_2^+) begins to appear. In the region below 1160 Å, a new type of structure appears, perhaps due to autoionization or selective predissociation. Not only is GeH_4^+ very weak, but it has only been observed in a relatively narrow wavelength region, between ~1080–1180 Å. This general behavior (weak parent ion, step structure, narrow window of observation) is very similar to that displayed by SiH_4^+ (SiH_4).[1] Both GeH_4^+ and SiH_4^+ would be very difficult to detect by electron impact mass spectrometry.

2. GeH_2^+ (GeH_4)

This is the first fragment ion. A detailed photoion yield curve of GeH_2^+ (GeH_4) in the threshold region is displayed

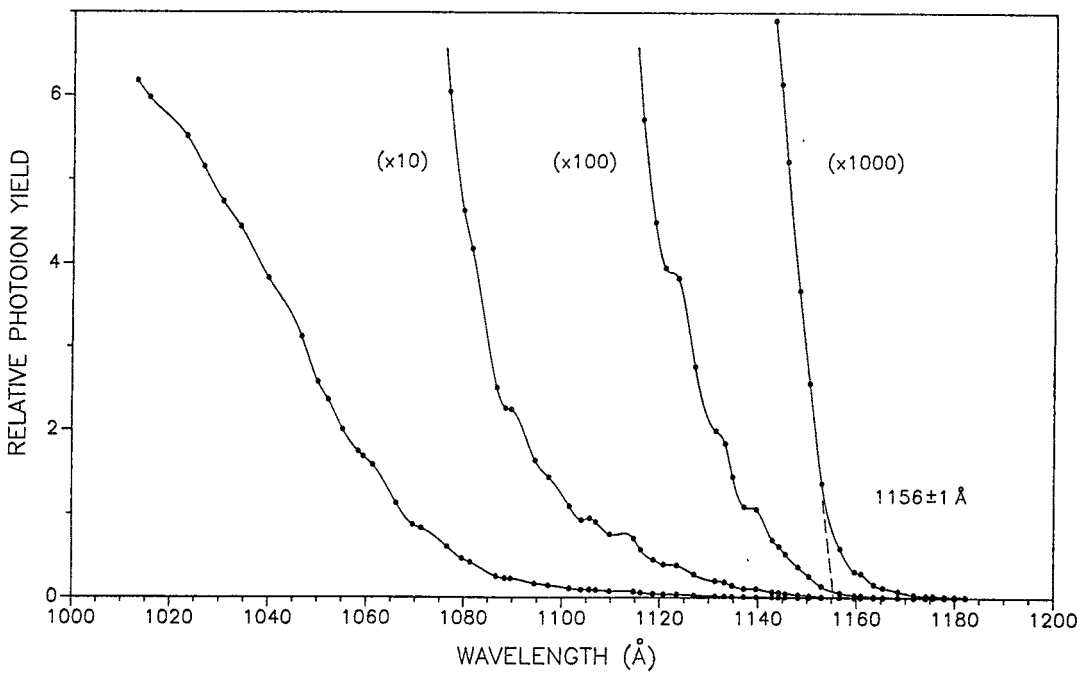

FIG. 3. The photoion yield curve of GeH_2^+ (GeH_4) near threshold.

in Fig. 3. Although its onset is below the adiabatic threshold observed in PES and hence it occurs in a weak Franck–Condon region, the approach to threshold is not far from linear. The extrapolated appearance potential is 1156 ± 1 Å $\equiv 10.72_5 \pm 0.009$ eV. When corrected for internal thermal energy of GeH_4 (1.097 kcal/mol at 300 K), the 0 K threshold becomes $10.77_2 \pm 0.009$ eV.

This value, and the other appearance potentials (A.P.) from GeH_4 obtained in this work, are summarized in Table I. Also listed in this table are the results of two studies[24,25] by electron impact mass spectrometry and two recent *ab initio* calculations.[18,27] As implied above, neither electron impact study detected GeH_4^+. More surprisingly, both electron impact measurements indicate that A.P.(GeH_3^+) is 1.0 eV lower than A.P.(GeH_2^+), whereas the present results (*vide infra*) and the *ab initio* calculations conclude that A.P.(GeH_2^+) < A.P.(GeH_3^+), by 0.76–0.9 eV. Kudo and Nagase[18] have calculated 4.9 kcal/mol for the enthalpy of the reaction

$$GeH_4^+ \rightarrow GeH_2^+ + H_2, \qquad (1)$$

whereas Binning and Curtiss[27] obtained 7.5 kcal/mol. Both calculations were performed at a fairly high level of theory. If we utilize our adiabatic ionization potential of GeH_4 and our appearance potential of GeH_2^+, we obtain 5.6 ± 0.5 kcal/mol for the endothermicity of reaction (1), in rather good agreement with both calculations.

3. GeH_3^+ (GeH_4)

Initial attempts at determining the threshold for this process were plagued by an extended region of curvature near the onset, encompassing at least 50 Å [Fig. 4(a)]. Various possible causes were examined, including gradually increasing Franck–Condon factors, scattered light, and pressure effects. Since GeH_2^+ (GeH_4) simulates the Franck–Condon effects in this region, an experiment was performed in which the ratio of intensities (GeH_3^+)/(GeH_2^+) was measured as a function of wavelength, with the anticipation that the gradually increasing ionization probability would be canceled in the ratio. This measurement [Fig. 4(b)] did, in fact, yield a much less curved function vs wavelength, but with a relatively high "background" ratio, more or less flat, at longer wavelengths. The experiment was repeated, with the GeH_4 pressure reduced by a factor of ~ 5. A similar curve was obtained [Fig. 4(c)]; however, the (GeH_3^+)/(GeH_2^+) ratio was reduced in the quasilinear region by about 10% and the background ratio diminished by a factor of 3–4. These observations implied that bimolecular collisional effects were playing a role. Collisional decomposition of GeH_4^+ could not be implicated, since the abundance of parent ion was too low to account for the tail in the photoion yield of GeH_3^+. It seems most likely that the ion–molecule reaction

$$GeH_2^+ + GeH_4 \rightarrow GeH_3^+ + GeH_3 \qquad (2)$$

is responsible for this background. Northrop and Lampe[25] report that this reaction has a rate constant of 2.8×10^{-10} cm^3 molecule s, i.e., it is very fast. We shall show below that this reaction is exothermic, by about 4 kcal/mol. An upper limit to the threshold for GeH_3^+ (GeH_4) extracted from Figs. 4(b) and 4(c) is 1068 ± 1 Å $\equiv 11.60_9 + 0.01$ eV, or $11.65_7 \pm 0.01$ eV at 0 K.

4. GeH^+ (GeH_4)

The process responsible for this ion is presumed to be

$$GeH_4 \rightarrow GeH^+ + H_2 + H + e. \qquad (3)$$

It is weak and has a threshold < 12.9 eV [see Fig. 1(b)]. The interesting aspect of this process is the relatively intense, broad peak centered at 15.5 eV and the autoionizing structure on the high energy side of this broad peak. A similar behavior was observed with SiH^+ (SiH_4),[1] but in the GeH^+ case, the peaks are much broader than the instrumental resolution and they display an asymmetric shape. The separation between peaks ($\sim 1560\ cm^{-1}$) and the general pattern (four relatively prominent peaks, one weaker one) are rather similar to the photoelectron spectrum of the inner band $(a_1)^{-1}$ of GeH_4 (see Fig. 1 and Ref. 21). From the adiabatic ionization potential (IP) reported for this band (18.21 eV) and the energy of the first autoionization peak in the GeH^+ photoionization spectrum, we calculate an effective quantum number $n^* = 2.503$. The uppermost occupied a_1 orbital in GeH_4 is expected to be primarily a 4*s*-like germanium orbital.[21] Rydberg transitions emanating from this orbital can be anticipated to be *p*-like in their quantum defect ($\delta = n - n^*$). The observations bear this out. The predict-

TABLE I. Appearance potentials of GeH_n^+ species from GeH_4 (eV).

		Electron impact		Calculation	
	Present data (0 K)	Saalfeld and Svec[a]	Northrop and Lange[b]	Kudo and Nagase[c]	Binning and Curtiss[d]
GeH_4^+	$\leqslant 10.53 \pm 0.02$	···	···	10.2	10.47
GeH_3^+	$\leqslant 11.65_7 \pm 0.01$	10.8 ± 0.3	10.9 ± 0.2	11.3	11.60
GeH_2^+	$10.77_2 \pm 0.009$	11.8 ± 0.2	11.9 ± 0.2	10.4	10.79
GeH^+	< 12.9	11.3 ± 0.3	11.2 ± 0.2	···	12.41
Ge^+	< 11.48	10.7 ± 0.2	10.4 ± 0.2	···	10.94

[a] Reference 24.
[b] Reference 25.
[c] Reference 18.
[d] Reference 27.

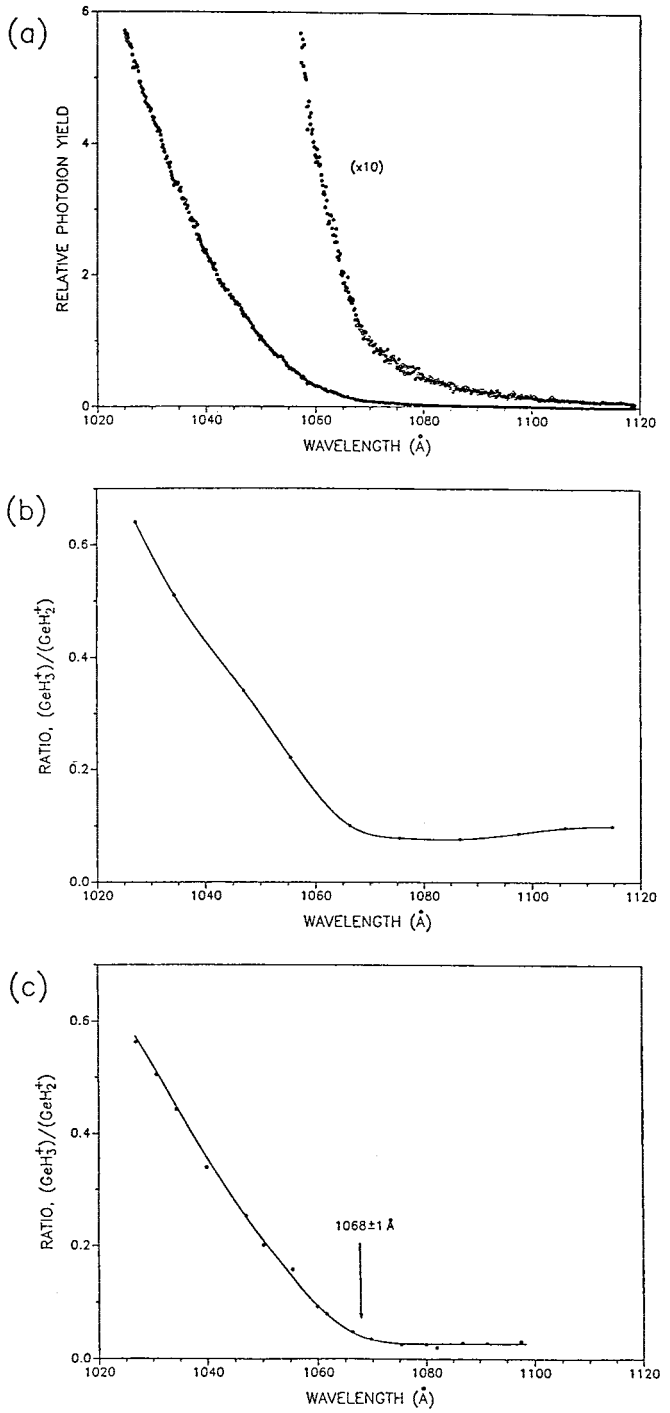

FIG. 4. (a) The photoion yield curve of GeH_3^+ (GeH_4), which displays a long, low energy tail due to collisional effects (see the text). (b) The ratio of ion intensities (GeH_3^+/GeH_2^+) from GeH_4, as a function of wavelength. The GeH_4 pressure is $\sim 10^{-4}$ Torr. (c) The same as (b), but with P (GeH_4) reduced by a factor ~ 5.

ed[26] p quantum defect for germanium is about 2.4 and thus n is close to 5. Consequently, the autoionization band in GeH^+ corresponds approximately to an $a_1 \rightarrow 5p$ transition. Bands with similar energies can be observed in GeH_2^+ and GeH_3^+. However, the fractional contribution of autoionization in these latter photoion yield curves is smaller, the peak energies are slightly different, and also the peak shapes.

5. Ge^+ (GeH_4)

The most likely origin of Ge^+ is the process

$$GeH_4 \rightarrow Ge^+ + 2H_2 + e. \quad (4)$$

It has a lower threshold than GeH^+, < 11.48 eV, and is more intense [see Fig. 1(b)]. There is less evidence for structure in this curve than in GeH^+. There are broad features, which are similar to those in GeH_3^+ and GeH_2^+, at ~ 13.5 and ~ 15.5 eV.

Due to the nature of these processes, the threshold of both Ge^+ and GeH^+ are regarded as upper limits and are not useful for thermochemical determinations.

B. Photoionization of the free radicals

1. GeH_3^+ (GeH_3)

The photoion yield curve of GeH_3^+ (GeH_3) is displayed in Fig. 5. Only the peaks in the hydrogen light source spectrum were employed in these measurements. Step structure is readily apparent in the region near threshold, with an average spacing of 8.83 Å $\equiv 393 \pm 15$ cm^{-1}. This is most probably the out-of-plane bending frequency excited in the transition from pyramidal GeH_3 to planar or near planar GeH_3^+. The adiabatic ionization potential is at least as low as 1560 ± 1 Å $\equiv 7.94_8 \pm 0.005$ eV. There is a still weaker feature at 1568 ± 1 Å $\equiv 7.90_7 \pm 0.005$ eV, but this may be a hot band. The GeH_3^+ photoion yield curve approaches a plateau at ~ 1380 Å and then increases rather sharply to ~ 1200 Å, beyond which it begins to decline. The more rapid increase in ion yield below ~ 1380 Å is suggestive of the onset of an excited state of GeH_3^+.

2. GeH^+ (GeH_3)

The GeH^+ fragment ion from photodissociative ionization of GeH_3 was measured at $m/e = 71$ as a function of wavelength and is shown in Fig. 6. The region near the onset (1380 ± 5 Å $\equiv 8.98 \pm 0.03$ eV) is extremely weak. A much sharper increase occurs below ~ 1285 Å. Assuming that the GeH_3 species has an internal energy corresponding to 300 K, we compute a 0 K threshold for GeH^+ (GeH_3) to occur at $\leqslant 9.02$ eV.

The sharp increase at $\lambda \leqslant 1285$ Å is again suggestive of an excited state of GeH_3^+ which readily decomposes into $GeH^+ + H_2$. A similar behavior (weak signal near threshold, more abrupt increase at higher energy) was observed in the corresponding photodissociative ionization process involving SiH_3.[1] No experimental data have yet been published on the first excited state of GeH_3^+ and SiH_3^+. Available calculations indicate that the formation of such an excited state should occur by single electron ejection from an e-type orbital, which allows for Jahn–Teller distortion. One may speculate that the more rapid increase in GeH^+ (GeH_3), and the corresponding increase in SiH^+ (SiH_3), occurs when a Jahn–Teller state is accessed which has a larger ionization and/or dissociative ionization probability.

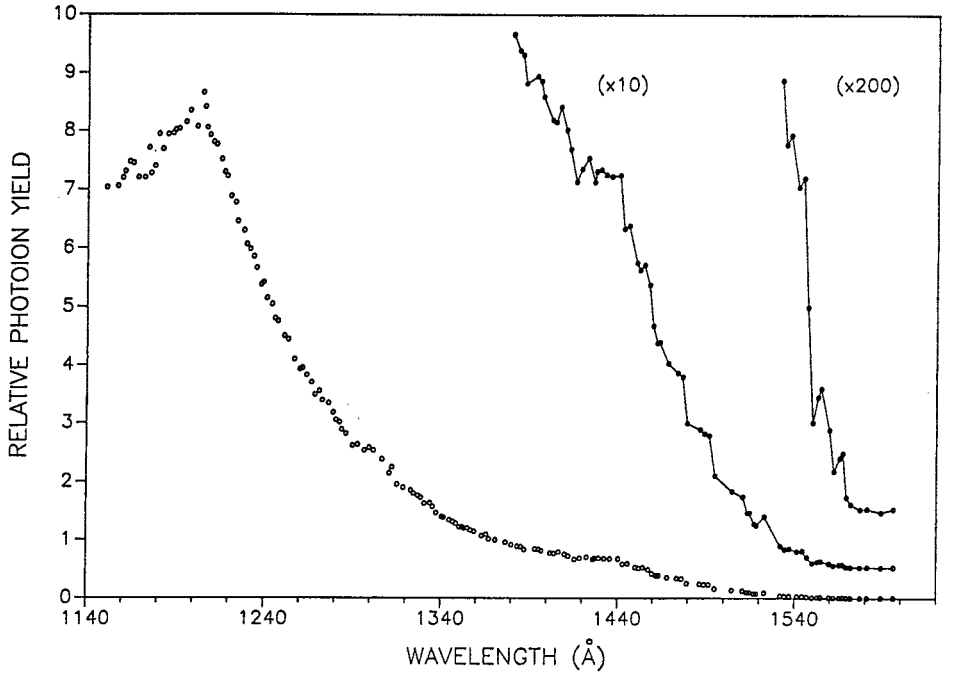

FIG. 5. The photoion yield curve of GeH_3^+ (GeH_3). The GeH_3 species is generated *in situ* by the $F + GeH_4$ reaction.

3. GeH_2^+ (GeH_2)

In the related study of the SiH_2 produced by the successive abstraction reactions with atomic fluorine, little difficulty was encountered in observing SiH_2^+ (SiH_2). In fact, evidence was presented for the formation and detection of both the $X\,^1A_1$ and $a\,^3B_1$ states of SiH_2. Since the Ge–H bonds are expected to be weaker than the Si–H bonds, it was anticipated that the detection of GeH_2^+ (GeH_2) would be straightforward. Instead, a weak signal was observed at $m/e = 72$, most of which was $^{72}Ge^+$, rather than $^{70}GeH_2^+$, as judged by a corresponding signal at $m/e = 70$ ($^{70}Ge^+$). The $m/e = 70$ signal was followed to longer wavelengths and was consistent with the presence of atomic germanium in the reaction vessel. In the corresponding SiH_4 reaction,[1] SiH^+ (SiH) could be detected, but not atomic silicon. We speculate that GeH_2 is generated in the $F + GeH_4$ reaction, but that most of it is decomposed upon collision with other molecules or on the wall, producing atomic germanium. A few such collisions are expected in our reaction cell before the species can exit through the 5 mm orifice. If GeH_2 is formed in both $X\,^1A_1$ and $a\,^3B_1$ states, and the branching ratio favors $a\,^3B_1$, this excited species may more readily decompose into $Ge + H_2$. A further indication of the rapid loss of GeH_2 is the absence of any detectable signal for GeH^+ (GeH). Presumably, GeH would be formed by the

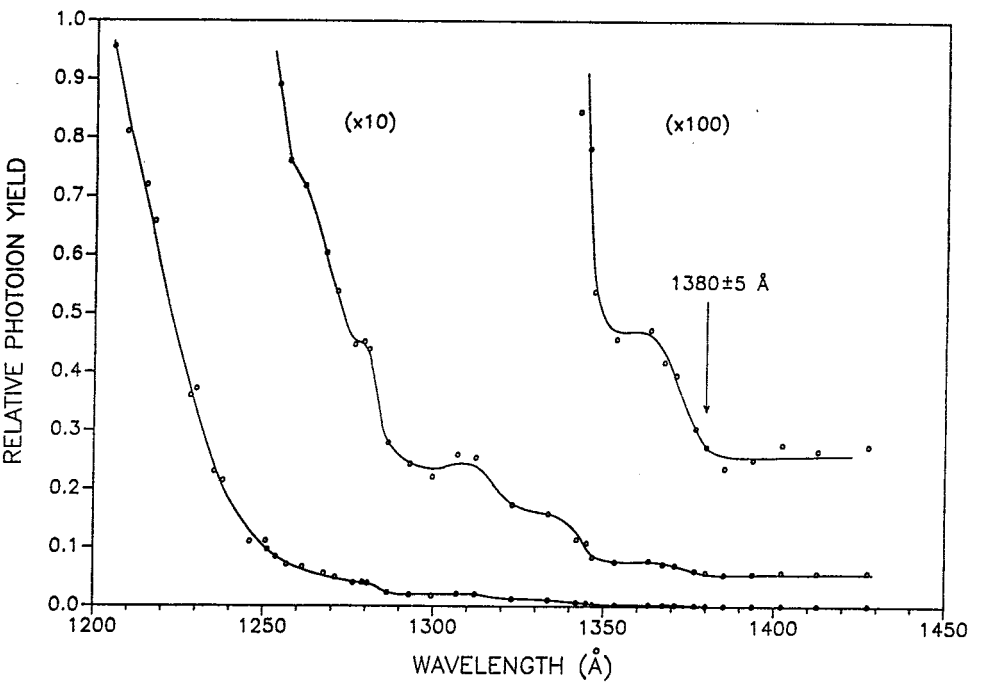

FIG. 6. The photoion yield curve of GeH^+ (GeH_3).

$F + GeH_2$ reaction; the weakness of the GeH_2 signal makes the probability of formation of GeH less likely.

Despite these difficulties, an upper limit to the adiabatic ionization potential of GeH_2 was obtained by laborious measurement of the signal at $m/e = 72$ as a function of wavelength. The ionization potential of atomic germanium is 7.8995 eV[28] ≡ 1569.5 Å. That of GeH_2 is expected to be considerably higher. One observes (Fig. 7) a somewhat higher value for this signal between 1200–1300 Å and then a rather rapid decline to ~1340 Å. The background to longer wavelength is attributable to $^{72}Ge^+$. Hence, the adiabatic ionization potential of GeH_2 is $\leqslant 9.25$ eV ≡ 1340 Å. A much better measurement could undoubtedly be performed with monoisotopic Ge, since the signal would be five times stronger and the background of atomic germanium would be absent.

The adiabatic ionization potentials of the GeH_n free radicals obtained in the current study are summarized in Table II. Also shown are the results of the recent *ab initio* calculations of Binning and Curtiss.[27]

IV. INTERPRETATION OF RESULTS

A. Thermochemistry

Gunn and Green[29] measured the heat of formation of GeH_4 at 298 K and obtained $+21.6 \pm 0.5$ kcal/mol. This value (for some reason, 21.7 kcal/mol was used) has been erroneously converted to 0 K in various compilations,[30,31] but a more nearly correct value 24.29 kcal/mol is given in the National Bureau of Standards tabulation.[32] The heat of formation of atomic germanium[3] (0 K) is 88.2 ± 0.7 kcal/mol and that of atomic hydrogen[2] is 51.634 kcal/mol. By combining these quantities in appropriate stoichiometric fashion, one obtains 270.5 ± 0.9 kcal/mol for the heat of atomization of GeH_4.

From the present measurements, an upper limit to the appearance potential of GeH_3^+ (GeH_4) is $11.65_7 \pm 0.01$ eV and the adiabatic ionization potential of GeH_3 is 7.94_8 eV. This leads to D_0 (H_3Ge–H) $\leqslant 3.70_9$ eV ≡ 85.5 kcal/mol. This value is almost certainly too high. The appearance potential of GeH_3^+ (GeH_4) is very likely shifted to higher energy, since GeH_3^+ is the second (higher energy) fragment. On the other hand, the value favored by Setser and co-workers,[4] 78.0 ± 1.0 kcal/mol, may well be a lower limit, although they regard it as an upper limit. These authors have reacted F, Cl, and O with GeH_4. The reaction of choice[4(a)] involved F atoms and the exoergicity of this reaction was determined by the maximum excitation of HF product. This was corrected for thermal energy ($3RT = 1.8$ kcal/mol) and an activation energy of 0.5 kcal/mol. However, in an earlier paper,[4(f)] in which the $F + GeH_4$ reaction was described, they note that if they "... ignore the contribution of thermal energy to the reaction D(H–GeH_3) $\leqslant$ 78.4 kcal/mol... ." Clearly, the higher the excitation observed in product HF, the weaker is the H_3Ge–H bond energy. However, if some of the HF excitation derives from the initial internal energy of GeH_4, a corrected value taking into account this internal energy would increase the derived value of D_0 (H_3Ge–H). The contribution of rotational energy may be most suspect. The B constant (inverse moment of inertia) of the spherical top GeH_4 molecule is 2.69 cm^{-1}, very nearly that (2.65 cm^{-1}) of the CD_4 molecule. The thermal distribution of rotational levels for a spherical top

$$N_J \sim (2J+1)^2 e^{-B(J)(J+1)/kT} \tag{5}$$

is given by Herzberg[33] for CD_4 at 300 K. One can see that, although the most probable value of J is about 10 ($E_{10} = 0.85$ kcal/mol), a substantial fraction of the molecules have $J \geqslant 15$ ($E_{15} = 1.85$ kcal/mol), and a not insignificant fraction have $J \geqslant 20$ ($E_{20} = 3.24$ kcal/mol). Hence, a possible interpretation of the chemiluminescence experi-

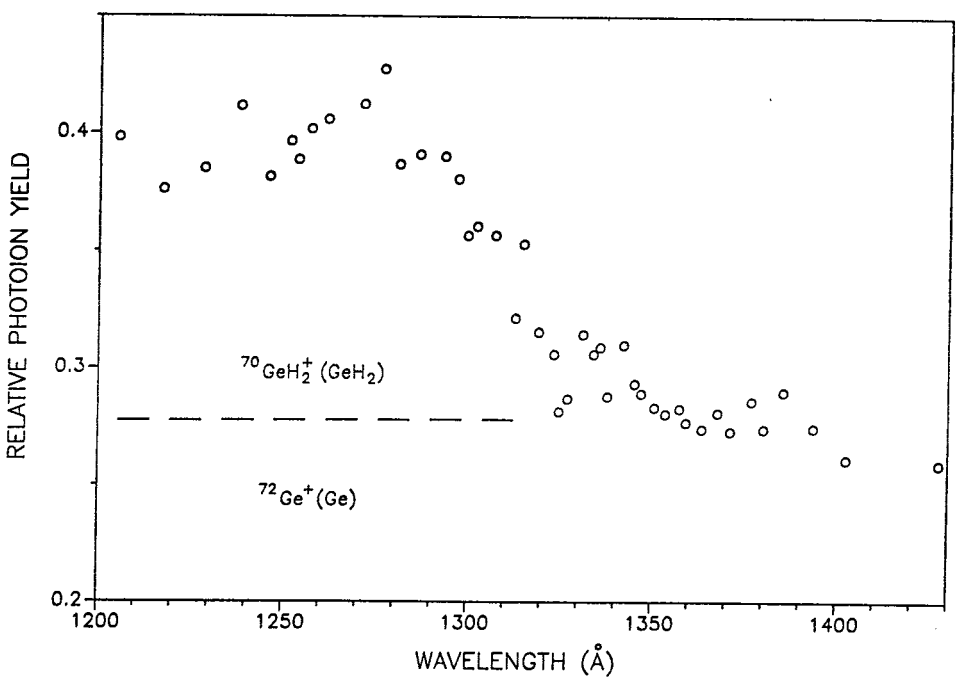

FIG. 7. The photoion yield curve of the $m/e = 72$ ion, generated in the $F + GeH_4$ reaction. This mass corresponds to $^{72}Ge^+$ and $^{70}GeH_2^+$. The decline to ~1335 Å corresponds to the onset region for $^{70}GeH_2^+$, the background to $^{72}Ge^+$.

TABLE II. Ionization thresholds from GeH_n free radicals (eV).

	Present work	Calculation[a]
$GeH_3 \rightarrow GeH_3^+ + e$	$\leqslant 7.94_8 \pm 0.005$	7.92
$GeH_3 \rightarrow GeH^+ + H_2 + e$	$\leqslant 9.02 \pm 0.03$	8.73
$GeH_2 \rightarrow GeH_2^+ + e$	$\leqslant 9.25$	9.09
$GeH \rightarrow GeH^+ + e$	...	7.67 (7.74[b])

[a] Reference 27.
[b] With spin–orbit correction.

ments would lead to D_0 (H_3Ge–H) $\cong$ 81 kcal/mol. We estimate that the kinetic shift in the appearance potential of GeH_3^+ (GeH_4) could be 3–4 kcal/mol, which would reduce D_0 (H_3Ge–H) from our upper limit of 85.5 to ~82 kcal/mol. Such a value would be in satisfactory agreement with the iodination results of Walsh and co-workers[5] 83 $\pm$ 2.4 kcal/mol. On this basis, our current best estimate is 82 $\pm$ 2 kcal/mol for D_0 (H_3Ge–H). This implies ΔH^0_{f0} (GeH_3) = 54.7 $\pm$ 2 kcal/mol.

The appearance potential of GeH_2^+ (GeH_4) reported in this study, $10.77_2 \pm 0.009$ eV, should be a fairly reliable quantity. The GeH_2^+ is the first fragment and the approach to threshold is not far from linear. However, the difficulties encountered in the measurement of GeH_2^+ (GeH_2) enable us to extract only an upper limit $\leqslant$9.25 eV for this adiabatic ionization potential. From this information, we can deduce $\Delta H_0 \geqslant 1.522$ eV $\equiv$ 35.1 kcal/mol for the decomposition reaction

$$GeH_4 \rightarrow GeH_2 + H_2. \quad (6)$$

Binning and Curtiss[27] have calculated 9.08 eV for the adiabatic ionization potential of GeH_2. With this value, the endothermicity of reaction (4) becomes 39.0 kcal/mol. This result is intriguingly close to the enthalpy inferred for thermal decomposition of germane to $GeH_2 + H_2$. Newman *et al.*[34] have performed shock tube studies and used Rice–Ramsberger–Kassel–Marcus (RRKM) theory to determine the activation energy for the forward (54.3 kcal/mol) and backward (15 $\pm$ 10 kcal/mol) reactions. The net decomposition energy is thus 39.3 $\pm$ 10 kcal/mol. Reference 5(b) cites unpublished work by Walsh which is equivalent to 35.3 $\pm$ 3 kcal/mol for this reaction. Devyatykh and Frolov[35] have obtained 37.5 kcal/mol for the activation energy of the heterogeneous decomposition of GeH_4 on a germanium film surface, which apparently acts as a catalyst for this reaction. While the mechanism of this latter decomposition is not clear, it may be that the rate determining step is the decomposition to $GeH_2 + H_2$. The GeH_2 product should readily decompose to Ge (solid) + H_2.

From the endothermicity of reaction (6), we conclude that $\Delta H_0 \geqslant 138.4$ kcal/mol and, more probably, 141 $\pm$ 2 kcal/mol for the reaction

$$GeH_4 \rightarrow GeH_2 + 2H. \quad (7)$$

With our choice of the H_3Ge–H bond energy, we infer $D_0(H_2Ge\text{–}H) > 56.4$ kcal/mol and more probably 59 kcal/mol. Hence ΔH^0_{f0} (GeH_2) $\geqslant$ 59.3 kcal/mol and, more probably, 61.8 kcal/mol.

We are left with about 129.6 kcal/mol (< 132.1 kcal/mol) to apportion to the remaining bond energies. Since GeH was not detected in the present experiments, our conclusions are of necessity more speculative and dependent in part on other sources. We have measured the threshold for the reaction

$$GeH_3 \rightarrow GeH^+ + H_2 \quad (8)$$

to be $\leqslant$9.02 eV. Binning and Curtiss[27] have calculated the adiabatic ionization potential of GeH and obtained 7.66 eV. This seems a plausible value, based on the following considerations. The ionization potential of CH (10.64 eV)[8] is 0.628 eV *less* than that of C (11.2676 eV).[36] The ionization potential of SiH (7.91 eV)[1] is 0.24 eV *less* than that of Si (8.1517 eV).[37] By extrapolating this trend, we anticipate that IP(GeH) will be less than that of Ge (7.8995 eV)[28] by an increment less than 0.24 eV. Also, we expect IP(GeH) to be less than IP(SiH). Accepting the value of Binning and Curtiss for IP(GeH), we can deduce $\Delta H_0 \leqslant 31.4$ kcal/mol for the reaction

$$GeH_3 \rightarrow GeH + H_2. \quad (9)$$

With our previously selected value for ΔH^0_{f0} (GeH_3), this enthalpy leads to ΔH^0_{f0} (GeH) $\leqslant$ 86 kcal/mol, or D_0(GeH) $\geqslant$ 2.33 eV.

Thus, 2.33 eV $\leqslant D_0$(GeH) $\leqslant$ 3.3 eV, the latter value being the upper limit established by a predissociation. The calculated and recommended value of Balasubramanian and Li,[10] 2.74 $\pm$ 0.05 eV, meets this criterion. At this time, it is the most reliable value for D_0 (GeH). With this choice, D_0(HGe–H) < 68.9 kcal/mol and, more probably, 66.4 kcal/mol. The heats of formation of the GeH_n and GeH_n^+ species deduced from the above analysis are summarized in Table III. The stepwise bond energies of GeH_{n-1}–H (n = 1–4) are listed in Table IV.

With the current data on GeH_n bond energies, the recently established SiH_n[1] and previously known CH_n,[3] it is useful to draw some comparisons. In order to normalize these observations, we divide each bond energy by the average bond energy for that system, i.e., 98.1, 75.7, and 67.7 kcal/mol for CH_4, SiH_4, and GeH_4, respectively. A plot of this fractional bond energy vs the type of bond (M–H, HM–H, etc.) appears in Fig. 8. It is immediately apparent that the pattern of GeH_n bonding is quite similar to that of SiH_n, but markedly different from CH_n. The H_2M–H bond is the weakest one in GeH_n and SiH_n, but the strongest in CH_n. Goddard and Harding have prefigured this qualitative behavior in their review article.[38] In particular, the decrease in

TABLE III. Heats of formation of GeH_n and GeH_n^+.

	Present work[a]	Setser and co-workers[b]	Walsh and co-workers[c]	Binning and Curtiss[d]
			ΔH^0_{f0} (GeH_n) (kcal/mol)	
GeH_4	(24.19)[e]	(24.19)[e]	(24.19)[e]	16.8[19.6]
GeH_3	<58.1 (54.7 ± 2)	50.6	55.2 ± 2.4	50.0[52.8]
GeH_2	$\geqslant 59.3$ (61.8)	...	60.4 ± 3.8	56.4[59.2]
GeH	$\leqslant 86$ (76.8)	...	...	74.9[76.0]
			ΔH^0_{f0} (GeH_n^+) (kcal/mol)	
GeH_4^+	267			258[261]
GeH_3^+	<241 (238)			232.6[235.4]
GeH_2^+	$\leqslant 272.6 \pm 0.2$			266.0[268.8]
GeH^+	<266			251.7[254.5]

[a] Quantities in parentheses are more probable values.
[b] Reference 4.
[c] Reference 5.
[d] Reference 27. Quantities in square brackets include an estimated spin–orbit correction.
[e] Based on $\Delta H^0_{f298} = 21.6 \pm 0.5$ kcal/mol from Ref. 28, corrected to 0 K.

bonding strength between HM–H and H_2M–H for SiH_n and GeH_n is attributed to the need for unpairing the spins (noting that both SiH_2 and GeH_2 have $^1A_1$ ground states), whereas this is not necessary for CH_2 (which has *a* $^3B_1$ ground state).

The strikingly similar pattern of SiH_n and GeH_n suggests that the big change occurs between first row and second row elements and that SnH_n bond strengths may be predicted by knowing the atomization energy and making use of Fig. 8. Thus, from ΔH_f (SnH_4) $= 41.8 \pm 0.5$ kcal/mol[29,32] and ΔH_f (Sn,*g*) $= 72.0 \pm 0.2$ kcal/mol,[3] the atomization energy is 236.7 ± 0.5 kcal/mol, or an average bond energy of 59.2 kcal/mol. Using Fig. 8, we estimate (kcal/mol) D_0(Sn–H) = 55, D_0(HSn–H) = 58, D_0(H_2Sn–H) = 51.5, and D_0(H_3Sn–H) = 71.6. The only experimental value available for comparison is D_0(Sn–H) $\leqslant$ 62.9 kcal/mol[8] based on an observed predissociation. However, a rather extensive relativistic quantum mechanical calculation[39] yields D_0(Sn–H) = 53 kcal/mol.

B. Implications from the thermochemical results

1. The ion–molecule reaction

The data contained in Table III enable us to evaluate the enthalpy of the ion–molecule reaction (2). The rigorous upper limit for ΔH^0_{f0}(GeH_3) and ΔH^0_{f0}(GeH_3^+) leads to $\Delta H^0_0 < -2.3$ kcal/mol, while the more probable values for these quantities yield $\Delta H^0_0 = -4.1$ kcal/mol. The evidence in our data for a background which is quadratic in pressure is consistent with reaction (2) being slightly exoergic and having no significant activation barrier. From data given in Ref. 1, the analogous reaction of SiH_2^+ with SiH_4 is exoergic by about 3 kcal/mol. This latter reaction has been measured[40] to have a rate constant $\geqslant 10^{-9}$ cm^3/molecule s, i.e., typical of

TABLE IV. Stepwise bond energies (kcal/mol, 0 K).

	Present study[a]	Setser and co-workers[b]	Walsh and co-workers[c]	Klynning and Lindgren[d]	Calculations
H_3Ge–H	$<85.5(82 \pm 2)$	78.0 ± 1.0	82.7 ± 2.4	...	84.8[e]
H_2Ge–H	$>56.4(59)$	...	56.9 ± 2.9	...	58.0[e]
H–Ge–H	$<68.9(66)$	...	...	...	70.2[e] [68.5]
Ge–H	$>53.7(63)$	...	...	<76.1	63.2 ± 1[f];64.9[e] [63.8]

[a] Quantities in parentheses are more probable values.
[b] Reference 4.
[c] Reference 5.
[d] Reference 9.
[e] Reference 27. Quantities in square brackets include an estimated spin–orbit correction.
[f] Reference 10.

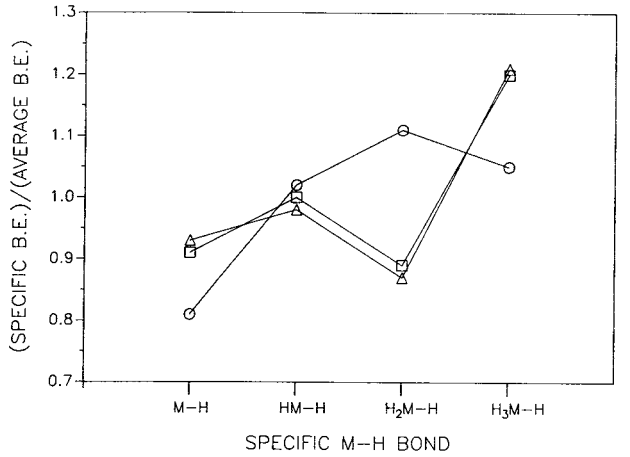

FIG. 8. The ratio of a particular bond energy to the average bond energy, plotted against the sequential bonds M–H, HM–H, H_2M–H, and H_3M–H, where $M = C$ (○); Si(□); and Ge(△).

an exoergic, very rapid ion–molecule reaction, which appears also to be the case for the $GeH_2^+ + GeH_4$ reaction.[25]

2. The presence of atomic germanium

In our earlier studies[1] on the reaction products from the $F + SiH_4$ reaction, we observed SiH_3, SiH_2 (both $X\,^1A_1$ and $a\,^3B_1$) and SiH, but no Si(g). In the present studies of the $F + GeH_4$ reaction, we observe GeH_3, some GeH_2, no GeH, but some Ge(g). Our interpretation of this difference in behavior is based on the relative stability of SiH_2 and GeH_2.

It is now fairly well established[1] that ΔH^0_{f0} (SiH_2) $= 65.6 \pm 2$ kcal/mol. The heat of formation of atomic silicon[3] is 106.5 ± 2 kcal/mol. Hence, we compute

$$SiH_2(X\,^1A_1) \rightarrow Si(g) + H_2, \quad \Delta H^0_{f0} = 40.9 \text{ kcal/mol}. \tag{10}$$

The $a\,^3B_1$ state of SiH_2, which lies 21.0 ± 0.7 kcal/mol[1] above $X\,^1A_1$, is still stable with respect to these decomposition products by 19.9 ± 2.8 kcal/mol. In the present work, we have established that $\Delta H^0_{f0}(GeH_2) \geqslant 59.35$ kcal/mol and, more probably, 61.8 kcal/mol. The heat of formation[3] of atomic germanium is 88.2 ± 0.7 kcal/mol. From this information, we compute

$$GeH_2 \rightarrow Ge(g) + H_2, \quad \Delta H^0_{f0} \leqslant 28.9 \text{ kcal/mol} \tag{11}$$

and, more probably, $\Delta H^0_{f0} = 26.4$ kcal/mol.

Several calculations[11–14] cited in the Introduction conclude that the ground state of GeH_2 is $^1A_1$ (as in SiH_2) and the $a\,^3B_1$ state lies 23 ± 2 kcal/mol above $^1A_1$. Hence, the current best estimate is that $GeH_2(A\,^3B_1)$ is barely stable with respect to Ge(g) + H_2. There is sufficient uncertainty in the ionization potential of GeH_2 and the singlet–triplet separation to allow for $GeH_2(a\,^3B_1)$ to be unstable. If this is the case, and if the accommodation coefficient of atomic germanium on the surface of our reaction chamber is significantly less than unity, then atomic germanium could survive and be detected in our experiment. This would appear to be a plausible explanation for the stated observations. It suggests that the reaction $F + GeH_3$ generates $GeH_2(a\,^3B_1)$ in at least comparable abundance to $X\,^1A_1$.

C. Structural implications

1. GeH_4^+

The weak intensity of GeH_4^+, and the very large (0.8 eV) difference between our observed adiabatic ionization potential and that deduced from photoelectron spectroscopy strongly support the conclusion of Kudo and Nagase,[18] i.e., GeH_4^+ in its ground state must have a structure very far from tetrahedral. Their conclusion that this GeH_4^+ structure looks like $GeH_2^+ \cdot H_2$, with C_s symmetry, is very similar to the earlier results[19,20] on SiH_4^+.

2. GeH_3^+

Neutral GeH_3 appears to be less pyramidal[41] (i.e., closer to planar) than SiH_3. Since the ground state of SiH_3^+ has been calculated to be planar, it is quite likely that the ground state of GeH_3^+ is also planar. The next deeper lying occupied orbital in both SiH_3 and GeH_3 has e symmetry. Single electron ejection from this orbital should produce the first excited state of the cation, which should be subject to Jahn–Teller distortion. The unusual behavior of the photoion yield curves in both SiH^+ (SiH_3) and GeH^+ (GeH_3), displaying a very gradual increase from threshold, and then (at higher energy) a more abrupt increase are believed to reflect the Franck–Condon probabilities in the excitation of pyramidal GeH_3 (SiH_3) to the Jahn–Teller distorted states.

V. CONCLUSIONS

The adiabatic ionization potential of GeH_4 has been measured to be $\leqslant 10.53$ eV (perhaps as low as 10.44 eV) much lower than the value (11.3 eV) obtained by photoelectron spectroscopy. The very weak GeH_4^+ signal between 10.5–11.3 eV implies a large Jahn–Teller distortion of GeH_4^+ from a tetrahedral structure. The appearance potential of GeH_2^+ (GeH_4) is $\leqslant 10.77_2 \pm 0.009$ eV; that of GeH_3^+ (GeH_4) is $< 11.65_7 \pm 0.01$ eV. The free radicals GeH_3 and GeH_2 have been generated by the $F + GeH_4$ reaction. The adiabatic ionization potential of GeH_3 is $7.94_8 \pm 0.005$ eV; that of GeH_2 is $\leqslant 9.25$ eV. The appearance potential of GeH^+ (GeH_3) is $\leqslant 9.02$ eV. These data, together with auxiliary information, lead to the following heats of formation in kcal/mol at 0 K (more probable values in parentheses):

$GeH_3 < 58.1$ (54.7 ± 2); $GeH_2 \geqslant 59.3$ (61.8);

$GeH \leqslant 86$ (76.8).

Corresponding values for the cations are

$GeH_4^+ = 267$; $GeH_3^+ < 241$ (238.5);

$GeH_2^+ \leqslant 272.6 \pm 0.2$; $GeH^+ < 266$.

The incremental bond energies (kcal/mol) deduced from these studies are $D_0(H_3Ge\text{–}H) < 85.5$ (82 ± 2), $D_0(H_2Ge\text{–}H) > 56.4$ (59), $D_0(HGe\text{–}H) < 68.9$ (66.3), and $D_0(GeH) > 53.7$ (63). The specific bond energy (normalized to average bond energy) in GeH_n is remarkably similar to that in SiH_n, but markedly different from that in CH_n. This observation is used to estimate the individual bond energies in SnH_n. The ion–molecule reaction $GeH_2^+ + GeH_4 \rightarrow GeH_3^+ + GeH_3$ is observed and inferred to be slightly exothermic. The prescence of Ge(g) and absence of GeH in the

$F + GeH_4$ reaction is interpreted to result from the instability of $GeH_2(a\,^3B_1)$ to decomposition into $Ge(g) + H_2$.

An autoionization band is observed in the GeH^+ (GeH_4) photoion yield curve (and also, less markedly, in GeH_2^+ and GeH_3^+) which is assigned to an $a_1 \rightarrow 5p$ transition in GeH_4.

ACKNOWLEDGMENT

This research was supported by the U.S. Department of Energy, Office of Basic Energy Sciences, under Contract No. W-31-109-ENG-38.

[1]J. Berkowitz, J. P. Greene, H. Cho, and B. Ruscic, J. Chem. Phys. **86**, 1235 (1987).
[2]M. W. Chase, Jr., C. A. Davies, J. R. Downey, Jr., D. J. Frurip, R. A. McDonald, and A. N. Syverud, J. Phys. Chem. Ref. Data **14**, Suppl. No. 1, 1–1856 (1985).
[3]V. P. Glushko, L. V. Gurvich, G. A. Bergman, I. V. Veits, V. A. Medvedev, G. A. Khachkuruzov, and V. S. Yungman, *Termodinamicheski Svoistva Individual'nikh Veshchestv* (Nauka, Moscow, 1979), Vol. 2.
[4](a) B. S. Agrawalla and D. W. Setser, J. Chem. Phys. **86**, 5421 (1987); (b) J. Phys. Chem. **90**, 3450 (1986); (c) M. A. Wickramaaratchi and D. W. Setser, *ibid.* **87**, 64 (1983); (d) J. P. Sung and D. W. Setser, J. Chem. Phys. **69**, 3868 (1978); (e) D. J. Bogan and D. W. Setser, *ibid.* **64**, 594 (1976); (f) K. C. Kim, D. W. Setser, and C. M. Bogan, *ibid.* **60**, 1837 (1974).
[5](a) M. J. Almond, A. M. Doncaster, P. N. Noble, and R. Walsh, J. Am. Chem. Soc. **104**, 4717 (1982); (b) P. N. Noble and R. Walsh, Int. J. Chem. Kinetics **15**, 547 (1983).
[6]K. J. Reed and J. I. Brauman, J. Chem. Phys. **61**, 4830 (1974).
[7]F. E. Saalfeld and H. J. Svec, J. Phys. Chem. **70**, 1753 (1966).
[8]K. P. Huber and G. Herzberg, *Molecular Spectra and Molecular Structure. IV. Constants of Diatomic Molecules* (Van Nostrand Reinhold, New York, 1979).
[9]L. Klynning and B. Lindgren, Ark. Phys. **32**, 575 (1966).
[10]K. Balasubramanian and J. Li, J. Mol. Spectrosc. **128**, 413 (1988).
[11]K. Balasubramanian, J. Chem. Phys. **89**, 5731 (1988).
[12]R. A. Phillips, R. J. Buenker, R. Beardsworth, P. R. Bunker, Per Jensen, and W. P. Kraemer, Chem. Phys. Lett. **118**, 60 (1985).
[13]G. Olbrich, Chem. Phys. Lett. **73**, 110 (1980).
[14]J.-C. Barthelat, B. Saint Roch, G. Trinqier, and J. Satge, J. Am. Chem. Soc. **102**, 4080 (1980).
[15]L. A. Curtiss and J. A. Pople, Chem. Phys. Lett. **88**, 1775 (1988).
[16]C. W. Bauschlicher, Jr., S. R. Langhoff, and P. R. Taylor, J. Chem. Phys. **87**, 387 (1987).
[17]K. Balasubramanian and A. D. McLean, J. Chem. Phys. **85**, 5117 (1986).
[18]T. Kudo and S. Nagase, Chem. Phys. Lett. **148**, 73 (1988).
[19]J. A. Pople and L. A. Curtiss, J. Phys. Chem. **91**, 155 (1987).
[20]R. F. Frey and E. R. Davidson, J. Chem. Phys. **89**, 4227 (1988).
[21]A. W. Potts and W. C. Price, Proc. R. Soc. London Ser. A **326**, 165 (1972).
[22]S. T. Gibson, J. P. Greene, and J. Berkowitz, J. Chem. Phys. **83**, 4319 (1985).
[23]P. De Bievre, M. Gallet, N. E. Holden, and I. L. Barnes, J. Phys. Chem. Ref. Data **13**, 809 (1984).
[24]F. E. Saalfeld and H. J. Svec, Inorg. Chem. **2**, 46 (1963).
[25]J. K. Northrop and F. W. Lampe, J. Phys. Chem. **77**, 30 (1973).
[26]J. Berkowitz, J. P. Greene, H. Cho, and G. L. Goodman, J. Phys. B **20**, 2647 (1987).
[27]R. C. Binning, Jr. and L. A. Curtiss, J. Chem. Phys. **92**, 1860 (1990), and private communication.
[28]C. M. Brown, S. G. Tilford, and M. L. Ginter, J. Opt. Soc. Am. **67**, 584 (1977).
[29]S. R. Gunn and L. G. Green, J. Phys. Chem. **65**, 779 (1961).
[30]National Bureau of Standards Technical Note 270-3 (U.S. GPO, Washington, D.C., 1968).
[31]H. M. Rosenstock, K. Draxl, B. W. Steiner, and J. T. Gerron, J. Phys. Chem. Ref. Data **6**, I-780 (1977).
[32]D. D. Wagman, W. H. Evans, V. B. Parker, R. H. Schumm, I. Halow, S. M. Bailey, K. L. Churney, and R. L. Nuttall, J. Phys. Chem. Ref. Data **11**, 114 (1982).
[33]G. Herzberg, *Molecular Spectra and Molecular Structure. II. Infrared and Raman Spectra* (Van Nostrand, New York, 1945), p. 40.
[34]C. G. Newman, J. Dzarnoski, M. A. Ring, and H. E. O'Neal, Int. J. Chem. Kinetics **12**, 661 (1980).
[35]G. C. Devyatykh and I. A. Frolov, Russ. J. Inorg. Chem. **11**, 385 (1966).
[36]C. E. Moore, *Atomic Energy Levels*, Natl. Stand. Ref. Data Ser. Natl. Bus. Stand. (U.S. GPO, Washington, D.C., 1971), Vol. 35.
[37]C. M. Brown, J. Opt. Soc. Am. **64**, 1665 (1974).
[38]W. A. Goddard III and L. B. Harding, Annu. Rev. Phys. Chem. **29**, 363 (1978).
[39]K. Balasubramanian and K. S. Pitzer, J. Mol. Spectrosc. **103**, 105 (1984).
[40]J. M. S. Henis, G. W. Stewart, M. K. Tripodi, and P. P. Gaspar, J. Chem. Phys. **57**, 389 (1972).
[41]G. S. Jackel, J. J. Christiansen, and N. Gordy, J. Chem. Phys. **47**, 4274 (1967).